

## Literature Review: Part II

**Project Title:** GHz Low Noise Amplifier Design for Optical Shot Noise Measurements

Week 2: 11<sup>th</sup> to 16<sup>th</sup> June 2018

IISER Summer Student Programme

**Project Guide:** Dr. Shouvik Datta

**Student name:** Rutwik Narendra Jain

## Contents

<b>1 Coherence: Qualitative [9], [1]</b>	<b>1</b>
1.1 Interference . . . . .	1
1.2 Young's Fringes: Spatial Coherence . . . . .	2
1.3 The Michelson Interferometer: Temporal Coherence . . . . .	3
<b>2 Coherence: Quantitative [1], [9]</b>	<b>5</b>
2.1 Michelson Interferometer . . . . .	5
<b>3 Photon Antibunching [1]</b>	<b>6</b>
3.1 Stellar and Intensity Interferometers . . . . .	6
3.2 HBT Experiments and classical description of $ g^2(\tau) $ . . . . .	7
3.3 HBT experiments with photons . . . . .	7
3.4 Relation between antibunching and sub-Poissonian photon statistics . . . . .	8

## 1 Coherence: Qualitative [9], [1]

- ✓ Real light is not monochromatic, but contains a range of frequencies. A single spectral line consists of a frequency range, its linewidth.
- ✓ A wave consisting of several frequencies is not fully predictable i.e. its behaviour contains randomness. Incoherence is a consequence of this randomness.
- ✓ Two wavetrains are coherent if their random variations are statistically correlated.
- ✓ Two separate waves may or may not be coherent with each other and an experimental test of coherence is to superpose them and look for 'stationary' interference.

### 1.1 Interference

Interference patterns generally occur when a light wave is divided and then recombined with a phase difference between the two paths.

Interference experiments are classified according to the way in which a beam of light is divided and recombined. Table 1, drawn from [9], is a concise reference.

### Link between coherence and ability to observe interference

Considering two waves having amplitudes  $U_1 = Ae^{i(\vec{k}_1 \cdot \vec{r} - \omega t)}$  and  $U_2 = Be^{i(\vec{k}_2 \cdot \vec{r} - \omega t - \alpha)}$ , where  $A, B \in \mathbb{R}$

The resultant amplitude and intensity after their interference or superposition at  $\vec{r}$  is

$$U_{\text{total}} = U_1 + U_2 = e^{i(\vec{k}_1 \cdot \vec{r} - \omega t)} \left[ A + Be^{i(\vec{k}_2 - \vec{k}_1) \cdot \vec{r} - i\alpha} \right]$$

$$\begin{aligned} \text{Intensity} \propto |U_{\text{total}}|^2 &= A^2 + B^2 + 2AB \cos \left[ (\vec{k}_2 - \vec{k}_1) \cdot \vec{r} - \alpha \right] \\ &= |U_1|^2 + |U_2|^2 + 2AB \cos \left[ (\vec{k}_2 - \vec{k}_1) \cdot \vec{r} - \alpha \right] \end{aligned}$$

Here, the cosine term is recognizable as interference, a positive or negative contribution to the resultant intensity that depends on the phases of the contributing waves.

When waves are coherent,  $k_1 = k_2 = k$  so that  $U_1 = Ae^{i(\vec{k} \cdot \vec{r} - \omega t)}$  and  $U_2 = Be^{i(\vec{k} \cdot \vec{r} - \omega t - \alpha)}$ , where  $A, B \in \mathbb{R}$  and  $\alpha$  is a constant.

$$U_{\text{total}} = e^{i(\vec{k} \cdot \vec{r} - \omega t)} \left[ A + Be^{-i\alpha} \right]$$

$$\begin{aligned} \text{Intensity} \propto |U_{\text{total}}|^2 &= A^2 + B^2 + 2AB \cos \alpha \\ &= |U_1|^2 + |U_2|^2 + 2AB \cos \alpha \cong |U_1|^2 + |U_2|^2 \end{aligned}$$

An ensemble average of random phase  $\alpha$  over values of 0 to  $2\pi$  will be zero as average of cosine over a period is zero  $\langle \cos \alpha \rangle_{0 \rightarrow 2\pi} = 0$ . The result is as if intensities should add instead of amplitude.

Table 1: Classification of interference experiments

<i>Description</i>	<i>Division of Wavefront</i>	<i>Division of Amplitude</i>
Example	Young's double slit experiment	Michelson Interferometer
Beam Properties	Small angular spread ( $\Delta\nu$ unimportant)	Small Bandwidth (collimation unimportant)
Requirement	Transverse (Spatial) Coherence	Longitudinal (Temporal) Coherence
	Sufficient coherence area	Sufficient coherence length/time
Quantitative	Cross-correlation function	Autocorrelation Function
	$\langle \mathcal{E}^*(\vec{r}_1, t) \mathcal{E}(\vec{r}_2, t + \tau) \rangle$	$\langle \mathcal{E}^*(\vec{r}_1, t) \mathcal{E}(\vec{r}_2, t + \tau) \rangle$

## 1.2 Young's Fringes: Spatial Coherence

The Young's double slit experiment does not require (almost does not) monochromaticity of the light used and can hence be said to have **tolerance to frequency range**. This is more because of what our eyes can 'see clearly' which depends on the allowable/detectable/permissible range of the order of interference  $p$  of the  $p^{\text{th}}$  fringe. Thus, as mentioned in 1, Young's double slit experiment is not concerned with what is called longitudinal or temporal coherence, that arises out of the inherent non-monochromaticity (existence of a  $\Delta\omega$ , detailed subsequently) of light from any real

light source. This is not of concern here, but there is another type of coherence called spatial or transverse coherence, that is concerned with the spread of angles within which light arrives to interfere.

**Q.** [Exercise 6.1 of Mark Fox] Show that the dark fringes from the centre of the source coincides with the bright fringes from the edges if  $D/L = \lambda/d$

**A.** With reference to figure 1,

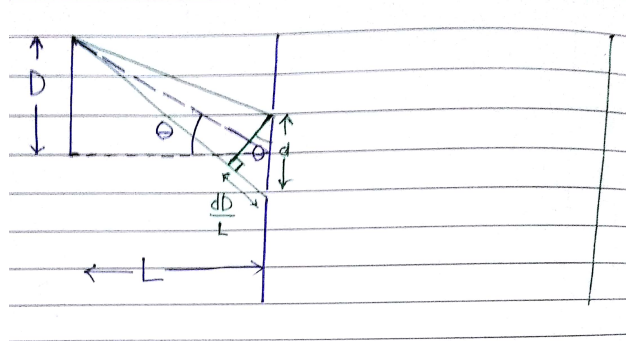


Figure 1: Double slit experiment with extended source

For light from the centre of the source,

$$x_{dark} = \frac{D'}{d}(2m+1)\frac{\lambda}{2}$$

For light from the end of the source, additional path difference is introduced as shown in the figure. Thus, at the same location  $x_{dark}$

$$\frac{x_{dark}d}{D'} + \frac{dD}{L} = n\lambda$$

$$\frac{D}{L} = \frac{\lambda}{2d} \quad m = n = 1$$

### 1.3 The Michelson Interferometer: Temporal Coherence

The Michelson intereferometer is shown in figure 1.3.

The 50:50 Beam Splitter (BS) divides the incident input light into two beams directed towards mirrors M1 and M2. While one beam traverses the distance  $2L_1$ , the other travels  $2L_2$  before recombining and giving the output at the viewing screen. The resultant electric field at output can be given by:

$$\mathcal{E}_{out} = \mathcal{E}_1 + \mathcal{E}_2 = \frac{1}{2}\mathcal{E}_0 e^{j2kL_1} + \frac{1}{2}\mathcal{E}_0 e^{j2kL_2} e^{j\Delta\phi}$$

$$\mathcal{E}_{out} = \frac{1}{2}\mathcal{E}_0 e^{j2kL_1} \left( 1 + e^{j2k(\Delta L)} e^{j\Delta\phi} \right) \quad (1)$$

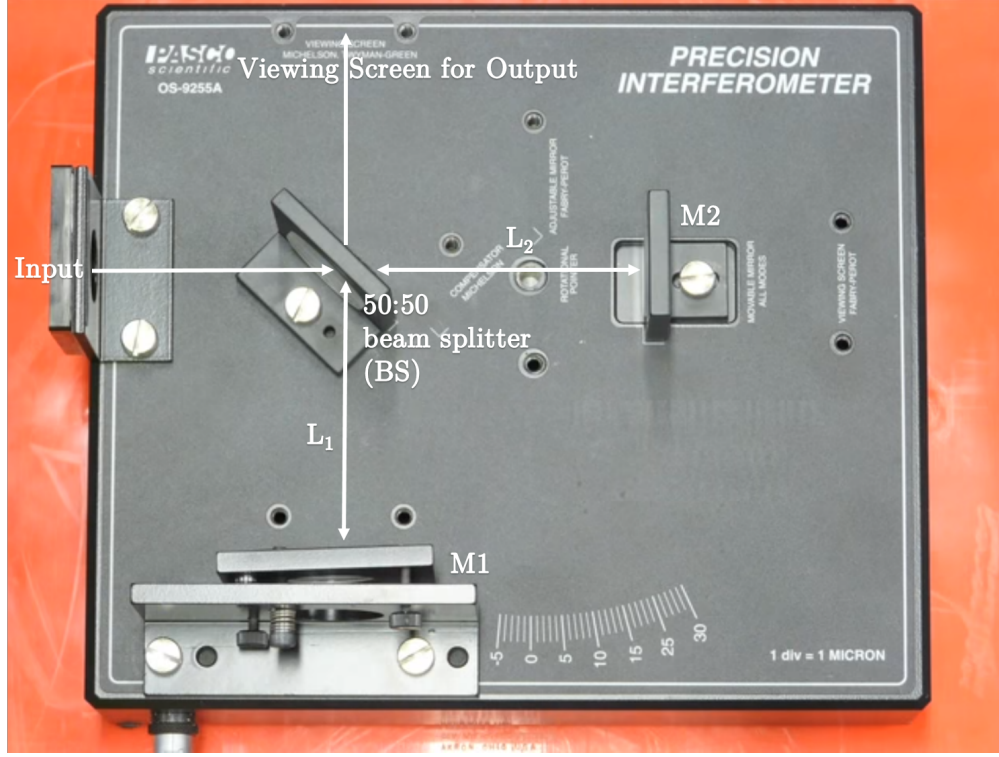


Figure 2: Michelson Interferometer setup

where  $\Delta L = L_2 - L_1$  is the path difference and  $k = 2\pi/\lambda$  is the wavenumber.

$\mathcal{E}_{out}$  is maximum if  $(e^{j2k(\Delta L)} e^{j\Delta\phi}) = 1 \Rightarrow \frac{4\pi}{\lambda} \Delta L + \Delta\phi = 2m\pi, m \in \mathbb{Z}^+$   
and minimum if  $(e^{j2k(\Delta L)} e^{j\Delta\phi}) = -1 \Rightarrow \frac{4\pi}{\lambda} \Delta L + \Delta\phi = (2m+1)\pi, m \in \mathbb{Z}^+$

Thus as  $L_2$  is scanned (or varied),  $\Delta L$  varies and bright and dark fringes appear alternately at the output with a period  $\lambda/2$ . The above analysis however assumes the frequency stability of light, when, in fact, all realistic sources contain a range of frequencies  $\Delta\omega$ .

As a direct consequence of the uncertainty principle and by de Broglie relation  $p = \hbar k = h/\lambda$ , an uncertainty in momentum  $\Delta p$  implies an uncertainty in  $\lambda$  or  $\omega$ .

The frequency spread of the sources imposes practical limits on the maximum path difference that will give observable fringes.

Summarising thus, the fringe pattern will be washed off in two cases:

- ✓ In the Young's double slit experiment, as shown before, due to limits on the spread of angles within which light reaches the point of superposition. (Spatial Coherence).

- ✓ In the Michelson interferometer, due to limits on frequency spread of the light source (Temporal Coherence).

## 2 Coherence: Quantitative [1], [9]

### 2.1 Michelson Interferometer

Coherence time  $\tau_c$  is defined as the time duration over which the phase of the wave remains stable. The coherence length  $L_c$  is defined as the length that the wavetrain covers over which the phase remains constant.

$$L_c = c\tau_c$$

Thus, if we know the phase of a wave at a position  $z$ , at  $t_1$  then the phase at the same position at time  $t_2$  will be known

with a high degree of certainty if  $|t_2 - t_1| \ll \tau_c$   
with a low degree of certainty if  $|t_2 - t_1| \gg \tau_c$

Alternatively, if we know the phase of a wave at some time  $t$ , and position  $z_1$  then the phase at the same time at position  $z_2$  will be known

with a high degree of certainty if  $|z_2 - z_1| \ll L_c$   
with a low degree of certainty if  $|z_2 - z_1| \gg L_c$

Thus, fringes will be observed in a Michelson interferometer only when

$$2\Delta L \ll L_c$$

The general result for experimental determination of  $\tau_c$  is by determining the spectral width of light.

$$\tau_c \approx \frac{1}{\Delta\omega} \quad (2)$$

A perfectly monochromatic source ( $\Delta\omega = 0$ ) has infinite  $\tau_c \Rightarrow$  perfect coherence.

The temporal coherence of light can be more accurately quantified by first-order correlation function, also called degree of first order coherence.

$$g^{(1)}(\tau) = \frac{\langle \mathcal{E}^*(t) \mathcal{E}(t + \tau) \rangle}{|\mathcal{E}(t)|^2} \quad (3)$$

where

$$\langle \mathcal{E}^*(t) \mathcal{E}(t + \tau) \rangle = \frac{1}{T} \int_T \mathcal{E}^*(t) \mathcal{E}(t + \tau) dt$$

- $|g^{(1)}(0)| = 1 \forall \phi$

- $|g^{(1)}(\tau)| = 1 \forall \tau \Leftrightarrow$  Light is perfectly coherent
- If  $0 \leq \tau \leq \tau_c \Rightarrow \phi(t + \tau) \cong \phi(t) \Rightarrow |g^{(1)}(\tau)|$  is close to unity  $\Rightarrow$  light is coherent.
- If  $\tau \gg \tau_c \Rightarrow \phi(t + \tau)$  and  $\phi(t)$  are uncorrelated  $\Rightarrow |g^{(1)}(\tau)| = 0$ .
- $|g^{(1)}(\tau)|$  drops from 1 to 0 on a time-scale of  $\tau_c$ .
- The visibility of fringe pattern in a Michelson interferometer  $= |g^{(1)}(\tau)|$

The second-order correlation function  $|g^{(2)}(\tau)|$  is the intensity analogue of the first-order correlation function. The nomenclature of 'second-order' arises from the relation that intensity of light is proportional to the second power of the electric field amplitude.

### 3 Photon Antibunching [1]

Apart from classification on the basis of photon statistics, light can also be classified on the basis of second-order correlation function  $|g^{(2)}(\tau)|$ , into three types - anti-bunched, coherent and bunched. Anti-bunched light is only possible in the photon interpretation, and is thus another proof for the quantum nature of light (just like the observation of sub-Poissonian photon statistics).

#### 3.1 Stellar and Intensity Interferometers

Just like the Young's fringes, which were washed out if light was not spatially coherent (in other words, limited by light's angular spread), the Michelson stellar interferometer, used for measuring diameters of stars, will form fringes in the focal plane of the telescope only if the light is spatially coherent.

In the setup, light from a bright star is collected by two mirrors separated by a distance  $d$ , and is directed through two slits into a telescope. Thus an interference pattern is formed (if the light is coherent) in the focal plane of the telescope.

As  $d$  is varied, the fringe visibility varies. Variation of fringe visibility with  $d$  enables the angular size of the star to be measured. If distance from the earth is known, the diameter can be calculated.

Angular spread of light source,  $\delta\theta_S = \frac{D}{L}$

Angular resolution of stellar interferometer,  $\delta\theta_R = 1.22\lambda/d$

By varying  $d$  and recording fringe visibility,  $\delta\theta_S$  can be determined and  $D$  can be evaluated as  $\delta\theta_S \times L$ .

As  $d \uparrow \Rightarrow \delta\theta_R \downarrow$  (improves). However, as  $d$  gets larger, it becomes difficult to stabilise the mirrors and observe a steady interference pattern.

The intensity interferometer, implemented by Hanbury and Twiss, overcomes the physical and stability limitations of the stellar interferometer. It measures the correlation between the photocurrents

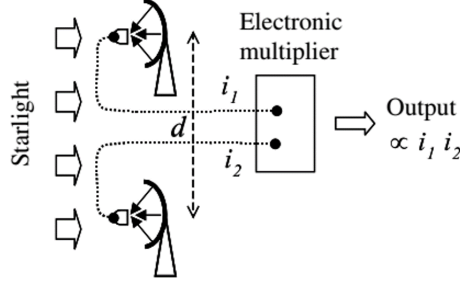


Figure 3: Intensity Interferometer

$i_1$  and  $i_2$  generated by the concentrated starlight that impinges on the two photomultipliers.

$$\text{Output} \propto \langle i_1 i_2 \rangle \propto I_1 I_2 \quad (4)$$

where  $I_1$  and  $I_2$  are intensities.

This correlation can be expressed in terms of the second-order correlation function.

### 3.2 HBT Experiments and classical description of $|g^{(2)}(\tau)|$

$$g^{(2)}(\tau) = \frac{\langle \mathcal{E}^*(t) \mathcal{E}^*(t+\tau) \mathcal{E}(t) \mathcal{E}(t+\tau) \rangle}{\langle \mathcal{E}^*(t) \mathcal{E}(t) \rangle \langle \mathcal{E}^*(t+\tau) \mathcal{E}(t+\tau) \rangle} = \frac{\langle I(t) I(t+\tau) \rangle}{\langle I(t) \rangle \langle I(t+\tau) \rangle} \quad (5)$$

- For perfectly monochromatic (idealized) light,  $g^{(2)}(\tau) = 1$ .
- If  $\tau \gg \tau_c$ ,  $I(t)$  and  $I(t+\tau)$  are uncorrelated with each other

$$\begin{aligned} \Rightarrow I(t) &= \langle I \rangle + \Delta I(t) \\ \langle I(t) I(t+\tau) \rangle_{\tau \gg \tau_c} &= \langle I \rangle^2 \\ \Rightarrow g^{(2)}(\tau \gg \tau_c) &= 1 \end{aligned}$$

- $g^{(2)}(0) \geq g^{(2)}(\tau)$
- $g^{(2)}(0) > 1$

### 3.3 HBT experiments with photons

Sometimes the photon picture concurs with the classical results and sometimes it does not. The key point relates to the time intervals between the photons in the light beam; that is, whether the photons come in bunches or whether they are regularly spread out. This naturally leads us to the concepts of bunched and antibunched light.

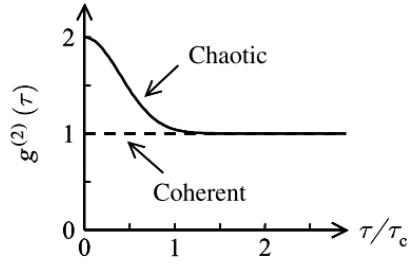


Figure 4: Classically allowed values of  $g^{(2)}(\tau)$

bunched light:  $g^{(2)}(0) > 1$ ,  
coherent light:  $g^{(2)}(0) = 1$ ,  
antibunched light:  $g^{(2)}(0) < 1$ .

In antibunched light the photons come out with regular gaps between them, rather than with a random spacing. The observation of photon antibunching is a purely quantum effect with no classical counterpart.

### 3.4 Relation between antibunching and sub-Poissonian photon statistics

Both phenomena are manifestations of certain non-classical states (or quantum nature) of light, that have no classical description.

Although these effects tend to occur together in most practical experiments carried out, both effects are distinct and **need not** occur together.

Surendra Singh (Opt. Commun. 44, 254 (1983)) showed that the photon-counting statistics can be either super- or sub-Poissonian, even though the photons always exhibit antibunching.

Zou and Mandel showed the opposite phenomenon is also possible i.e. the counting statistics can be sub-Poissonian when the photons exhibit bunching in time.

**Sub-Poisson counting statistics need not be associated with antibunching but can be accompanied by bunching. Therefore, sub-Poisson statistics and antibunching are distinct effects.**



## References

- [1] Mark Fox, Quantum Optics: An Introduction, Oxford Publications.
- [2] X. T. Zou, L. Mandel, Photon-anti-bunching and sub-Poissonian photon statistics, Physical Review A, Volume 41, Number 1, 1 January 1990.
- [3] Sergio Franco, Design with Operational Amplifiers and Analog Integrated Circuits, (Chapter 7, Noise), Third Edition, Tata McGraw Hill Publishing Company Ltd.
- [4] Dennis V. Perepitsa, Johnson Noise and Shot Noise, MIT, Department of Physics, November 27, 2006.
- [5] Johnson Noise and Shot Noise: The Determination of the Boltzmann Constant, Absolute Zero Temperature and the Charge of the Electron, MIT Department of Physics, September 3, 2013.
- [6] H. Nyquist, Thermal Agitation of Electric Charge in Conductors, Physical Review, Volume 32, July 1928.
- [7] Frank Rice, A frequency-domain derivation of shot-noise, Am. J. Phys. 84 (1), pp. 44-51, January 2016.
- [8] 1 MHz, Single-Supply, Photodiode Amplifier Reference Design, Texas Instruments.
- [9] Carlo Beenakker and Christian Schonenberger, Quantum Shot Noise: Fluctuations in the flow of electrons signal the transition from particle to wave behavior. Physics Today, page 37, May 2003.
- [10] Geoffrey Brooker, Modern Classical Optics, Oxford Publications.